

# The Mayari-Baracoa Paired Ophiolite Belt, Eastern Cuba: Implications for Tectonic Settings and Platinum-Group Elemental Mineralization

MEI-FU ZHOU,

*Department of Earth Sciences, University of Hong Kong, Hong Kong, China*

JOHN LEWIS,

*Department of Geology, George Washington University, Washington, District of Columbia, 20052*

JOHN MALPAS,

*Department of Earth Sciences, University of Hong Kong, Hong Kong, China*

AND NICOLAS MUNOZ-GOMEZ

*Departamento de Geologia, Instituto Superior Minero Metalurgico de Moa, Moa, Cuba*

## Abstract

The Jurassic Mayari-Baracoa ophiolite belt and associated Cretaceous volcanic rocks form the Zaza zone of eastern Cuba. This zone has been traditionally considered allochthonous and overrides a passive continental margin, the Cuban foreland. The ophiolites consist of mantle tectonites and cumulates, overlain by a volcanic-arc sequence including porphyritic basalts and andesitic lavas. These are, in turn, overlain by a sequence of tuffs and epiclastic sedimentary rocks. There are two ophiolitic massifs in the belt, the Mayari-Cristal Massif (MCM) and the Moa-Baracoa Massif (MBM). The MCM consists of harzburgites and dunites with abundant high-Cr podiform chromitites and dikes of gabbro and pyroxenite. The MBM, on the other hand, is composed of harzburgites with abundant high-Al podiform chromitites, cut by troctolite dikes. The two ophiolitic massifs have different REE and PGE patterns and contents. The mantle sequence in the MCM is more depleted than that in the MBM. We suggest that the MCM formed beneath a volcanic island arc and the MBM beneath a nascent spreading center in a back-arc basin. The two massifs form a paired ophiolite belt.

## Introduction

IN EASTERN CUBA, Mesozoic ophiolitic massifs contain typical podiform chromite deposits of high-Cr and high-Al varieties (Thayer, 1942, 1969; Guild, 1947; Kovacs et al., 1997; Proenza et al., 1997, 1999a, 1999b). Thayer's early observations of these deposits have been the basis of many of the presently accepted ideas on the origin of podiform chromitites. Among these deposits are the high-Cr (metallurgic) type in the Mayari-Cristal Massif (MCM) and the high-Al (refractory) type in the Moa-Baracoa Massif (MBM) (Proenza et al., 1999b). Each massif has different petrological and geochemical features. The question arises: are the mantle sequences of the two massifs essentially parts of a continuous sequence, perhaps sampled at different depths, or completely separate and different mantles formed in distinct tectonic settings? Proenza et al.

(1999b) proposed that both massifs represent the same mantle, and the formation of the chromite deposits was a consequence of mixing of various, hydrous melts at different places (depths) in the upper mantle. However, our study demonstrates that the mineralogical and bulk-rock chemical differences between the MCM and MBM reflect their formation in distinct tectonic settings. In addition, we report an extremely PGE-rich high-Cr chromitite in the MCM. All available data support the view that both the MCM and MBM represent paired ophiolite belts formed in adjacent suprasubduction-zone environments.

## Geological Background and Petrography

The Mayari-Baracoa ophiolite belt is part of the E-W-trending Cuban ophiolite belt that extends for more than 1000 km in the northern part of Cuba

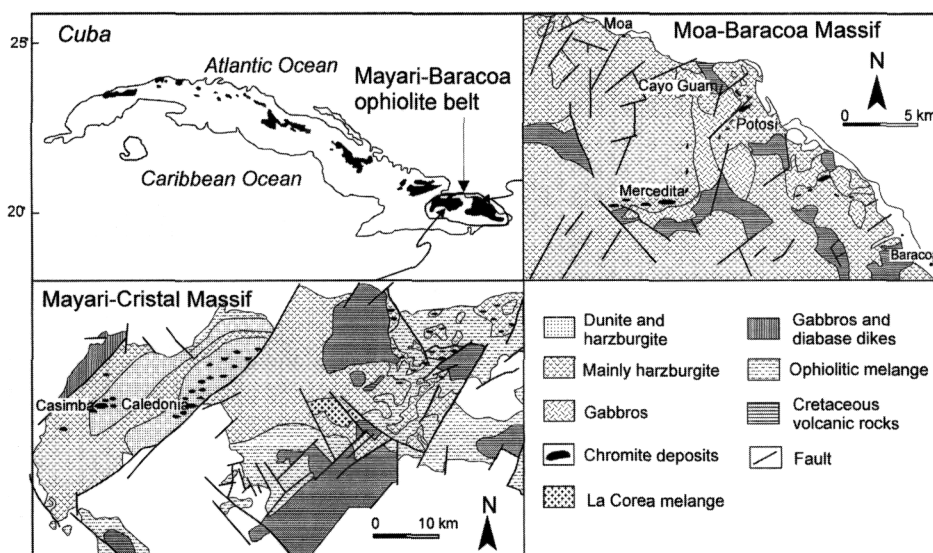


FIG. 1. Geological map of the Mayari-Baracoa ophiolite belt, eastern Cuba (after Proenza et al., 1999b).

(Fig. 1). The ophiolites are thought to be Late Jurassic–Early Cretaceous in age and have been traditionally considered allochthonous upon a passive continental margin sequence, the Cuban foreland (Iturralde-Vinent, 1996; Cobiella-Reguera, 2000). In eastern Cuba, the ophiolite thrust sheet is up to 1 km thick and rests subhorizontally on Cretaceous backarc volcanoclastics (Iturralde-Vinent, 1996).

The main features of the Mayari-Baracoa ophiolite belt and associated chromite deposits have been summarized by Proenza (1998, 1999). The ophiolite belt extends for 170 km, with a width of 10–20 km, and consists of two large allochthonous massifs—the MCM and MBM (Fig. 1). These massifs consist of ultramafic rocks and mafic cumulates, overlain by a volcanic-arc sequence of Cretaceous age, including porphyritic and amygdaloidal basalts with intercalations of pyroclastics, tuffs, cherts, and limestones. These are, in turn, overlain by a sequence of tuffs and epiclastic sedimentary rocks of Tertiary age.

The rocks of the MCM are mainly harzburgites with dunites and pyroxenite dikes. These are overthrust by microgabbros and diabase dikes. There are two large chromite deposits (Caledonia and Casimba) with more than 200,000 tons of metallogenic-grade ore, and at least 37 additional minor deposits. Chromite pods occur within dunites, and are subcon-

cordant with respect to the foliation in the host rocks. Chromitites are mainly nodular, disseminated, or massive. Serpentine, chlorite, and uvarovite are the main minerals in the matrix to the chromitites.

In the MBM, mantle tectonites consist of partly serpentinized harzburgite grading upward to a transition zone of harzburgites, dunites, plagioclase-peridotites, and gabbroic rocks. These rocks are cut by abundant dikes of troctolite and pegmatitic gabbro. The crustal sequence includes varitextured gabbros, microgabbros, dolerite, and diabase dikes, which are overlain by pillowed basalts and sedimentary rocks. The MBM has more than 100 chromite deposits of refractory-grade ore. Most are of small size, the Mercedita mine being the largest, but total ore reserves are more than 100,000 tons. Chromite pods always occur within a transition zone of serpentinites below a section of layered gabbro. The ultramafic rocks in the transition zone are mainly harzburgite and dunite, but there are also considerable amounts of plagioclase-bearing lithologies including plagioclase-dunite and harzburgite, and troctolites. The transition-zone ultramafic rocks are cut by numerous gabbroic dikes, many of which are pegmatic in nature, with plagioclase and clinopyroxene grains up to 0.5 meters in size. The dikes range in width from less than 1 cm to several meters, and are more abundant in chromitites than in the

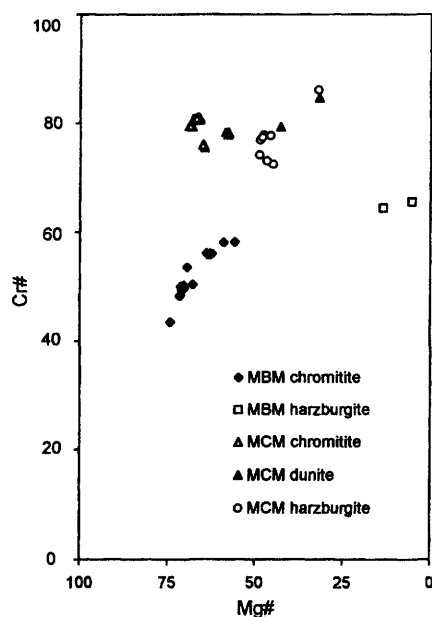


FIG. 2. Cr# [100Cr/(Cr+Al)] versus Mg# [100Mg/(Mg+Fe<sup>2+</sup>)] of chromites from the Mayari-Baracoa ophiolite belt, eastern Cuba.

peridotites. The pegmatic gabbros form a matrix to the chromitite and may include large broken fragments and crystals of chromite. Guild (1947) noted the occurrence of feldspathic "layers" within the chromite ore deposits, producing a mineral assemblage of chromite-plagioclase-olivine.

### Analytical Methods

Chemical compositions of both silicates and chromite were obtained using a JEOL JXA8800 microprobe. Analytical conditions were: accelerating voltage 15 kV and beam current 2 nA. We made use of a range of natural and synthetic standards and the manufacturer's ZAF correlation program. The accuracy of major oxides is better than 1 to 2%, whereas that of trace elements is between 2 and 10%.

Bulk-rock major oxides were analyzed with a Phillips PW2400 sequential X-ray fluorescence spectrometer using fused glass disks (analytical accuracy better than 5%). To determine trace elements (Ni, Cu, Zn, Co, and V), samples were put into solution following a Na<sub>2</sub>O<sub>2</sub> sinter technique to circumvent potential problems associated with incomplete dissolution of chromite. The final solution was analyzed by AAS. The accuracy of these determinations is between 5 and 10%. Trace elements also

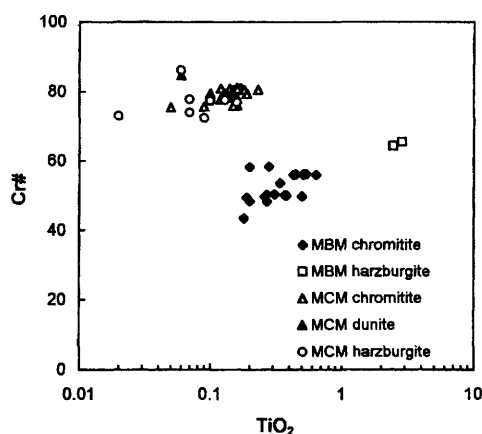


FIG. 3. Cr# [100Cr/(Cr+Al)] versus TiO<sub>2</sub> of chromites from the Mayari-Baracoa ophiolite belt, eastern Cuba.

were measured by XRF on pressed powder pellets, and there is good agreement between the results from these two methods.

PGE and Au contents were obtained following Ni-sulfide fire-assay preconcentration. The preconcentration used a combination of NiS fusion and Te coprecipitation. After preconcentration, the sample solutions were analyzed using a VG Elemental Plasma-quad 3 (PQ3) ICP-MS. This method is essentially the same as that described by Sun et al. (1993) and Zhou et al. (1998). Standard reference materials, WPR-1 and TDB-1, were analyzed a number of times during the analytical procedure. Analytical precision is better than 15% for Ru and Rh, and 10% for Ir, Pd, and Pt. Os data are not reported in this study, as it is difficult to control the loss of the Os oxides during sample preparation.

## Results

### Mineral chemistry

Representative compositions of chromite from the chromitites as determined by microprobe are presented in Table 1. As documented in Proenza et al. (1999b), chromites from the two massifs show different chemical compositions. Chromitites in the MCM contain chromite with higher Cr# than those of the MBM. In the Mg# versus Cr# plot (Fig. 2), chromitite in the MCM is typical of the high-Cr metallurgic variety, whereas the chromitite from the MBM is typical of the high-Al variety. The former chromites also have lower TiO<sub>2</sub> contents than the latter (Fig. 3). Chromites from both chromitites con-

TABLE 1. Chemical Compositions of Chromite from the Mayari-Baracoa Ophiolite Belt, Eastern Cuba<sup>1</sup>

Sample no.	TiO <sub>2</sub>	Cr <sub>2</sub> O <sub>3</sub>	Al <sub>2</sub> O <sub>3</sub>	MgO	FeO	Fe <sub>2</sub> O <sub>3</sub>	CaO	MnO	NiO	ZnO	Total	Cr#	Mg#
Moa-Baracoa Massif													
Chromitite													
CMM7	0.50	39.01	26.49	17.87	13.47	2.61	0.00	0.00	0.18	0.00	100.13	50	70
	0.38	39.16	26.29	17.97	13.05	2.56	0.01	0.12	0.20	0.18	99.92	50	71
	0.37	39.24	26.27	18.23	13.19	2.74	0.00	0.00	0.18	0.07	100.29	50	71
	0.31	39.53	26.14	17.25	14.62	2.62	0.02	0.00	0.13	0.03	100.65	50	68
CMM8-1	0.45	42.51	22.36	15.29	16.52	2.51	0.00	0.00	0.25	0.00	99.89	56	62
	0.43	42.66	22.59	15.64	16.03	2.48	0.04	0.04	0.27	0.11	100.30	56	64
	0.54	42.76	22.42	15.44	16.32	2.48	0.03	0.00	0.30	0.01	100.30	56	63
	0.51	42.35	22.42	15.52	16.32	2.59	0.03	0.00	0.20	0.13	100.07	56	63
	0.52	43.06	22.51	15.76	15.98	2.49	0.02	0.00	0.34	0.00	100.68	56	64
	0.64	42.60	22.48	15.40	16.46	2.52	0.02	0.00	0.12	0.00	100.23	56	63
CMM10	0.27	39.54	26.25	17.97	13.55	2.67	0.01	0.00	0.23	0.03	100.52	50	70
	0.26	39.15	26.62	17.92	13.21	2.50	0.03	0.00	0.37	0.03	100.09	50	71
	0.19	39.01	26.86	18.11	13.20	2.58	0.02	0.00	0.35	0.10	100.42	49	71
	0.20	38.27	27.49	18.34	13.19	2.68	0.00	0.08	0.25	0.04	100.54	48	71
	0.27	38.42	27.65	18.37	13.05	2.59	0.02	0.00	0.29	0.08	100.74	48	72
	0.18	34.61	30.26	19.84	12.37	3.19	0.03	0.00	0.28	0.05	100.81	43	74
CMM11	0.20	44.40	21.40	13.76	17.19	1.79	0.01	0.10	0.22	0.07	99.14	58	59
	0.34	41.87	24.36	17.01	13.41	2.15	0.00	0.00	0.33	0.03	99.50	54	69
	0.28	44.42	21.33	12.94	18.42	1.73	0.00	0.22	0.23	0.00	99.56	58	56
Harzburgite													
CMM20-1	2.44	32.52	12.10	3.54	40.66	7.31	0.05	0.24	0.35	0.25	99.46	64	13
	2.86	23.00	8.14	1.59	50.57	11.68	0.12	0.32	0.35	0.11	98.74	65	5.3
Mayari-Cristal Massif													
Chromitite													
Cma1	0.05	58.09	12.66	13.81	13.57	0.57	0.02	0.00	0.18	0.00	98.95	75	65
	0.16	58.63	12.40	13.97	13.52	0.62	0.08	0.05	0.23	0.05	99.71	76	65
	0.09	58.45	12.60	13.79	13.57	0.52	0.06	0.00	0.18	0.04	99.29	76	64
Cma5	0.15	58.32	12.39	14.13	13.55	0.77	0.02	0.00	0.13	0.03	99.49	76	65
	0.16	61.04	9.82	14.15	13.14	0.82	0.05	0.00	0.15	0.00	99.32	81	66
	0.14	61.40	9.70	14.36	13.25	0.94	0.00	0.00	0.18	0.00	99.97	81	66
	0.17	61.45	9.65	14.38	12.98	0.87	0.00	0.00	0.25	0.05	99.81	81	66
	0.17	61.08	9.66	13.94	12.89	0.65	0.09	0.00	0.24	0.02	98.75	81	66
	0.17	61.21	9.77	14.35	12.91	0.84	0.04	0.00	0.18	0.05	99.52	81	67
	0.15	60.78	9.84	14.62	12.59	0.94	0.00	0.00	0.31	0.00	99.23	81	67
	0.16	62.07	9.69	14.25	12.98	0.70	0.03	0.00	0.20	0.03	100.11	81	66
	0.16	61.61	9.68	14.38	12.81	0.79	0.05	0.00	0.22	0.00	99.70	81	67
	0.23	61.05	9.91	14.61	13.07	1.03	0.00	0.00	0.22	0.00	100.12	81	67
	0.16	61.43	9.77	14.76	12.57	0.93	0.05	0.00	0.32	0.00	99.99	81	68
	0.18	61.79	10.03	14.30	12.79	0.63	0.02	0.00	0.07	0.09	99.90	81	67

(table continues)

TABLE 1. *Continued*

Sample No.	TiO <sub>2</sub>	Cr <sub>2</sub> O <sub>3</sub>	Al <sub>2</sub> O <sub>3</sub>	MgO	FeO	Fe <sub>2</sub> O <sub>3</sub>	CaO	MnO	NiO	ZnO	Total	Cr#	Mg#
Cma7	0.12	60.93	9.65	14.34	12.66	0.83	0.04	0.00	0.14	0.08	98.79	81	67
	0.10	60.81	10.55	14.93	11.98	0.76	0.07	0.00	0.29	0.02	99.52	79	69
	0.19	60.74	10.58	14.66	12.25	0.70	0.00	0.00	0.20	0.03	99.35	79	68
Cma9	0.13	61.04	10.54	14.99	12.22	0.84	0.03	0.00	0.13	0.10	100.01	80	69
	0.15	57.50	10.64	12.49	16.31	1.23	0.04	0.02	0.18	0.09	98.65	78	58
	0.16	58.48	11.04	12.68	16.65	1.21	0.00	0.00	0.19	0.00	100.41	78	58
	0.12	57.31	10.95	12.63	16.39	1.29	0.06	0.02	0.22	0.00	98.99	78	58
Dunite													
Cma12	0.13	57.71	10.72	12.65	15.96	1.16	0.04	0.00	0.08	0.07	98.52	78	59
	0.10	56.24	9.82	9.10	21.67	1.38	0.07	0.00	0.18	0.12	98.68	79	43
	0.06	57.12	6.93	6.73	25.82	1.87	0.03	0.00	0.20	0.21	98.98	85	32
Harzburgite													
Cma13	0.06	56.84	6.15	6.80	25.82	2.13	0.07	0.05	0.15	0.26	98.33	86	32
	0.07	57.21	10.95	10.01	19.70	0.88	0.06	0.07	0.18	0.10	99.23	78	48
	0.16	57.07	11.53	10.27	19.44	0.83	0.03	0.12	0.11	0.31	99.87	77	49
	0.10	57.28	11.23	10.10	19.51	0.79	0.06	0.03	0.11	0.24	99.45	77	48
Cma15	0.13	57.69	11.14	9.64	20.45	0.79	0.04	0.06	0.19	0.15	100.28	78	46
	0.09	53.02	13.57	9.72	21.30	1.26	0.05	0.00	0.25	0.01	99.28	72	45
	0.02	53.55	13.28	10.02	20.43	1.14	0.00	0.00	0.24	0.02	98.69	73	47
	0.07	55.08	12.92	10.42	19.52	0.93	0.05	0.00	0.18	0.21	99.37	74	49

<sup>1</sup>Mg# = 100Mg<sup>2+</sup>/(Mg<sup>2+</sup> + Fe<sup>2+</sup>), Cr# = 100Cr/(Cr + Al).

tain very small amounts of ZnO (<0.11 wt%) and similar amounts of NiO (about 0.2 wt%) (Table 1).

In the MBM, accessory chromites in harzburgites have Cr# ranging from 64 to 65, whereas chromites in harzburgites from the MCM have higher Cr# (72–86). Compositions of chromites in dunites are similar to those in chromites in each massif, except that they have lower Mg# (Figs. 2 and 3).

Compositions of the silicate minerals are given in Table 2. Olivines in chromitites have very high Fo contents and high NiO (0.40 wt%). Orthopyroxenes of harzburgites from the MCM massif have lower Al contents (Al<sub>2</sub>O<sub>3</sub> 0.77–0.95 wt%) than those of harzburgites from the MBM (Al<sub>2</sub>O<sub>3</sub> 1.93 wt%). Clinopyroxenes in harzburgites from the MBM have Al<sub>2</sub>O<sub>3</sub> contents of 2.7 to 3.27 wt% (Table 2). Plagioclases impregnated in a harzburgite (CMM20-1) of the MBM has compositions of CaO 13.3 wt% and Na<sub>2</sub>O 3.63 wt%—i.e., labradorite.

### Bulk-rock chemistry

As expected from chemical compositions of chromite, chromitites from the MBM have higher Al<sub>2</sub>O<sub>3</sub> but lower Cr<sub>2</sub>O<sub>3</sub> contents than their equivalents from the MCM at given SiO<sub>2</sub> contents (Table 3). The chromitites from both massifs have similar Cu and Zn contents. V contents of chromitites in the two massifs are higher than the silicate rocks (Fig. 4).

Chromitites from both the MBM and MCM have similar Ni, PGE, Au, and Cu patterns in mantle-normalized plots (Fig. 5). Both have positive Ru and negative Pt anomalies. In the MCM, dunites have a slightly positive Ru anomaly and a negative Pt anomaly, whereas the harzburgites have relatively flat PGE patterns. In the MBM, both the dunites and harzburgites have similar PGE patterns, and do not show Ru and Pt anomalies (Fig. 5). Harzburgites from the MCM are depleted in Rh and Pt, compared to those from the MBM.

TABLE 2. Chemical Compositions of Silicate Minerals<sup>1</sup> from the Mayari-Baracoa Ophiolite Belt, Eastern Cuba<sup>2</sup>

Sample no.		SiO <sub>2</sub>	TiO <sub>2</sub>	Cr <sub>2</sub> O <sub>3</sub>	Al <sub>2</sub> O <sub>3</sub>	MgO	FeO	CaO	Na <sub>2</sub> O	K <sub>2</sub> O	MnO	NiO	ZnO	Total	Fo
Olivine															
Moa-Baracoa massif															
Chromitite	CMM1	40.86	0.02	0.06	0.00	49.31	9.59	0.00	0.00	0.00	0.09	0.36	0.00	100.29	90.2
		41.20	0.00	0.01	0.00	49.57	8.40	0.00	0.01	0.00	0.12	0.36	0.00	99.67	91.3
		40.65	0.02	0.06	0.00	49.58	9.55	0.02	0.01	0.01	0.09	0.41	0.00	100.40	90.2
		40.51	0.00	0.04	0.00	48.87	9.23	0.00	0.00	0.00	0.10	0.35	0.00	99.10	90.4
	CMM8-1	40.25	0.04	0.00	0.00	49.09	8.59	0.00	0.04	0.00	0.13	0.41	0.04	98.59	91.1
		40.53	0.07	0.00	0.00	49.53	8.13	0.00	0.02	0.01	0.15	0.27	0.00	98.71	91.6
		41.03	0.01	0.02	0.00	49.86	7.95	0.00	0.01	0.00	0.15	0.25	0.00	99.28	91.8
		40.81	0.00	0.00	0.00	50.89	5.80	0.03	0.00	0.02	0.12	0.47	0.00	98.14	94.0
		40.76	0.06	0.01	0.00	51.12	5.94	0.06	0.06	0.02	0.11	0.43	0.00	98.57	93.9
		41.02	0.06	0.02	0.00	51.20	5.87	0.00	0.04	0.00	0.08	0.42	0.00	98.71	94.0
		41.42	0.00	0.03	0.00	51.41	6.61	0.05	0.02	0.00	0.05	0.43	0.00	100.02	93.3
Harzburgite	CMM20-1	39.09	0.00	0.25	0.00	41.02	18.80	0.07	0.00	0.05	0.21	0.41	0.00	99.90	79.5
		39.02	0.02	0.02	0.00	41.68	18.02	0.05	0.04	0.00	0.26	0.34	0.00	99.45	80.5
		38.63	0.07	0.03	0.00	41.28	18.28	0.02	0.02	0.01	0.22	0.20	0.00	98.76	80.1
		38.79	0.02	0.00	0.00	41.75	18.02	0.03	0.02	0.01	0.31	0.38	0.00	99.33	80.5
		38.94	0.00	0.00	0.00	41.11	18.62	0.08	0.28	0.00	0.26	0.40	0.00	99.69	79.7
Mayari-Cristal massif															
Dunite	Cma12	40.96	0.00	0.00	0.00	50.41	7.10	0.05	0.01	0.03	0.15	0.44	0.01	99.16	92.7
		40.69	0.03	0.00	0.00	50.35	7.23	0.06	0.03	0.02	0.10	0.46	0.00	98.97	92.5
		40.57	0.00	0.00	0.00	50.34	6.99	0.03	0.00	0.00	0.12	0.48	0.00	98.53	92.8
		40.52	0.02	0.00	0.00	50.48	7.18	0.08	0.00	0.00	0.13	0.46	0.02	98.89	92.6
Harzburgite	Cma13	40.66	0.02	0.04	0.00	49.70	7.88	0.02	0.00	0.00	0.14	0.40	0.02	98.88	91.8
		40.40	0.00	0.02	0.00	50.18	8.15	0.08	0.00	0.04	0.09	0.32	0.00	99.28	91.7
		40.78	0.01	0.00	0.00	49.83	8.13	0.08	0.00	0.00	0.12	0.38	0.01	99.34	91.6
	Cma15	40.84	0.00	0.00	0.00	49.66	8.69	0.05	0.03	0.00	0.16	0.56	0.03	100.02	91.1
		56.71	0.00	0.21	0.85	33.94	5.84	0.81	0.00	0.00	0.13	0.08	0.02	98.59	91.2
		40.65	0.00	0.00	0.00	49.46	8.92	0.00	0.00	0.00	0.17	0.45	0.00	99.65	90.8
		42.14	0.06	0.01	0.00	47.94	8.14	0.09	0.02	0.01	0.13	0.41	0.00	98.95	91.3
Clinopyroxene															
Moa-Baracoa massif															
Harzburgite	CMM20-1	52.08	0.57	0.76	2.70	16.06	5.09	21.70	0.48	0.00	0.16	0.08	0.00	99.68	
		51.52	0.61	1.00	3.27	16.61	5.95	19.69	0.24	0.00	0.23	0.00	0.00	99.12	
Orthopyroxene															
Mayari-Crital massif															
Harzburgite	Cma15	56.52	0.03	0.59	0.86	33.68	5.65	1.41	0.28	0.00	0.14	0.06	0.00	99.22	
		56.50	0.00	0.50	0.88	33.87	5.83	0.93	0.15	0.00	0.14	0.08	0.00	98.88	
		56.06	0.00	0.33	0.79	34.44	6.20	0.77	0.18	0.00	0.17	0.07	0.01	99.02	
		56.70	0.00	0.38	0.82	33.49	5.65	1.38	0.25	0.00	0.18	0.00	0.00	98.85	
		57.29	0.02	0.51	0.95	33.87	5.61	1.55	0.16	0.00	0.07	0.05	0.00	100.08	
		56.76	0.00	0.43	0.77	33.64	5.64	1.18	0.21	0.00	0.07	0.11	0.00	98.81	
Moa-Baracoa massif															
Harzburgite	CMM20-1	54.94	0.26	0.46	1.93	28.98	11.44	1.80	0.00	0.00	0.30	0.05	0.00	100.16	

<sup>1</sup>Olivine, clinopyroxene, and orthopyroxene.<sup>2</sup>Fo = 100 Mg<sup>2+</sup>/(Mg<sup>2+</sup> + Fe<sup>2+</sup>), and Fe<sup>2+</sup> is calculated from total FeO.

TABLE 3. Chemical Compositions of the Chromitites and Silicate Rocks from the Mayari-Baracoa Ophiolite Belt, Eastern Cuba<sup>1</sup>

Massif: Rock: Sample:	Mayari-Cristal massif										Moa-Baracoa massif																		
	Chromitite					Dunite					Harzburgite					Chromitite					PL-Dunite					Harzburgite			
	Cma1	Cma2	Cma3	Cma4	Cma5	Cma7	Cma12	Cma13	Cma15	Cma16	Cma17	Cma1	Cma2	Cma3	Cma4	Cma5	Cma7	Cma9	Cma10	Cma11	Cma13	Cma14	Cma18	Cma16	Cma17				
Major oxides (wt%)																													
SiO <sub>2</sub>	10.9	13.6	29.1	18.0	10.6	1.0	54.5	52.8	55.0	8.3	3.2	3.2	3.8	1.1	13.5	4.5	2.0	1.5	60.3	60.8	59.8								
TiO <sub>2</sub>	0.24	0.26	0.23	0.33	0.33	0.33	0.14	0.15	0.13	0.28	0.29	0.35	0.45	0.52	0.29	0.46	0.30	0.45	0.24	0.14	0.14								
Al <sub>2</sub> O <sub>3</sub>	13.4	10.6	7.0	17.3	8.8	13.3	0.1	0.8	0.5	20.3	27.9	28.0	27.4	29.7	23.2	25.8	27.2	28.3	7.3	0.9	0.5								
Fe <sub>2</sub> O <sub>3</sub>	4.08	3.21	3.63	1.42	2.97	4.34	4.52	7.18	6.60	3.54	2.42	3.41	4.57	6.87	2.46	2.85	4.01	4.22	9.38	9.42	10.3								
FeO	7.40	8.93	7.09	8.20	7.01	7.12	4.62	3.08	3.36	9.02	9.53	7.26	8.11	7.51	8.12	7.25	8.03	8.79	1.11	1.12	1.32								
MgO	27.4	33.7	35.9	31.7	37.6	25.4	54.8	52.2	47.7	35.5	31.2	31.9	26.8	22.9	34.9	28.9	24.2	24.1	39.0	44.9	43.8								
CaO	0.40	0.24	1.14	1.00	0.43	0.34	0.17	0.29	0.14	7.09	0.24	0.10	0.58	0.87	0.08	3.08	1.71	0.43	0.10	0.12	0.11								
MnO	0.03	0.04	0.07	0.03	0.04	0.06	0.12	0.13	0.14	0.08	0.04	0.05	0.04	0.04	0.03	0.03	0.04	0.02	0.12	0.11	0.11								
Cr <sub>2</sub> O <sub>3</sub>	40.2	34.2	24.7	27.8	38.3	49.3	0.2	0.5	0.4	21.4	27.9	28.9	30.0	34.7	24.5	29.2	32.8	34.1	0.5	0.5	0.5								
LOI*	4.67	6.03	9.45	6.61	6.56	4.39	16.6	15.0	12.6	8.19	3.32	3.79	2.44	4.70	7.26	2.57	0.93	2.31	15.5	15.7	14.8								
Trace elements (ppm)																													
Ni	821	1246	6421	1261	1440	653	2826	2718	2368	1212	1009	1103	908	813	1096	704	608	626	2202	2544	1514								
Cu	9.67	9.95	8.28	2.47	5.03	7.17	6.20	3.09	21.98	13	7.01	6.82	134	6.8	11.1	6.7	9.0	6.6	12.3	3.3	96								
Co	8.65	11.58	42.20	12.62	11.71	50.76	88.24	88.14	83.47	42.92	30.29	48.43	42.96	50.22	46.63	42.26	41.67	16.48	78.2	89.7	89.8								
V	616	507	451	456	609	919	35	29	22	439	599	726	506	802	554	708	742	763	35	23	85								
Zn	28	218	353	47	23	105	73	42	147	820	65	104	143	159	93	110	123	65	91	66	100								
Se	0.12	0.12	0.11	0.15	0.13	0.09	0.14	0.19	0.14	0.17	0.17	0.12	0.15	0.14	0.15	0.19	0.12	0.08	0.24	0.30	0.02								
S	20	99	134	108	126	131	849	1301	275	116	98	75	200	121	115	81	132	765	113	830	100								
Platinum-group elements (ppb)																													
Ru	51.1	5956	63.8	67.1	69.9	89.8	17.5	9.4	9.2	26.6	25.1	20.8	34.0	28.8	23.2	22.7	31.8	38.1	12.6	9.5	12.1								
Rh	6.27	131.6	6.98	3.18	7.03	8.12	0.60	1.38	1.13	0.89	0.84	0.78	1.15	0.71	0.77	0.48	0.77	1.20	1.47	1.40	1.50								
Pd	2.07	3.91	3.27	4.98	2.32	1.61	3.99	5.85	10.33	4.53	5.38	4.09	3.21	2.46	2.94	4.55	6.68	5.74	11.50	7.58	13.4								
Ir	28.0	2068	22.4	18.5	18.5	27.3	8.2	6.2	5.1	6.0	5.9	4.9	7.1	5.8	4.8	5.5	7.9	8.6	4.3	4.7	5.2								
Pt	1.95	53.10	1.55	1.60	0.89	0.71	2.33	3.35	9.07	1.22	1.96	1.46	0.16	0.26	1.39	1.03	0.89	1.02	7.19	8.21	8.95								
Au	1.03	1.79	1.30	2.17	2.01	1.50	2.77	2.77	4.46	5.10	4.63	3.15	3.06	2.37	2.92	3.33	6.43	4.52	2.90	3.43	4.50								
Pd/Ir	0.074	0.002	0.15	0.27	0.13	0.06	0.49	0.94	2.01	0.75	0.91	0.83	0.45	0.43	0.61	0.83	0.84	0.67	2.66	1.61	2.58								
Ni/Cu	85	125	775.33	510.03	286.15	91.166	455	878	108	91	144	162	6.76	120	98	105	68	95	179	780	16								

<sup>1</sup>LOI = loss on ignition; PL = plagioclase.

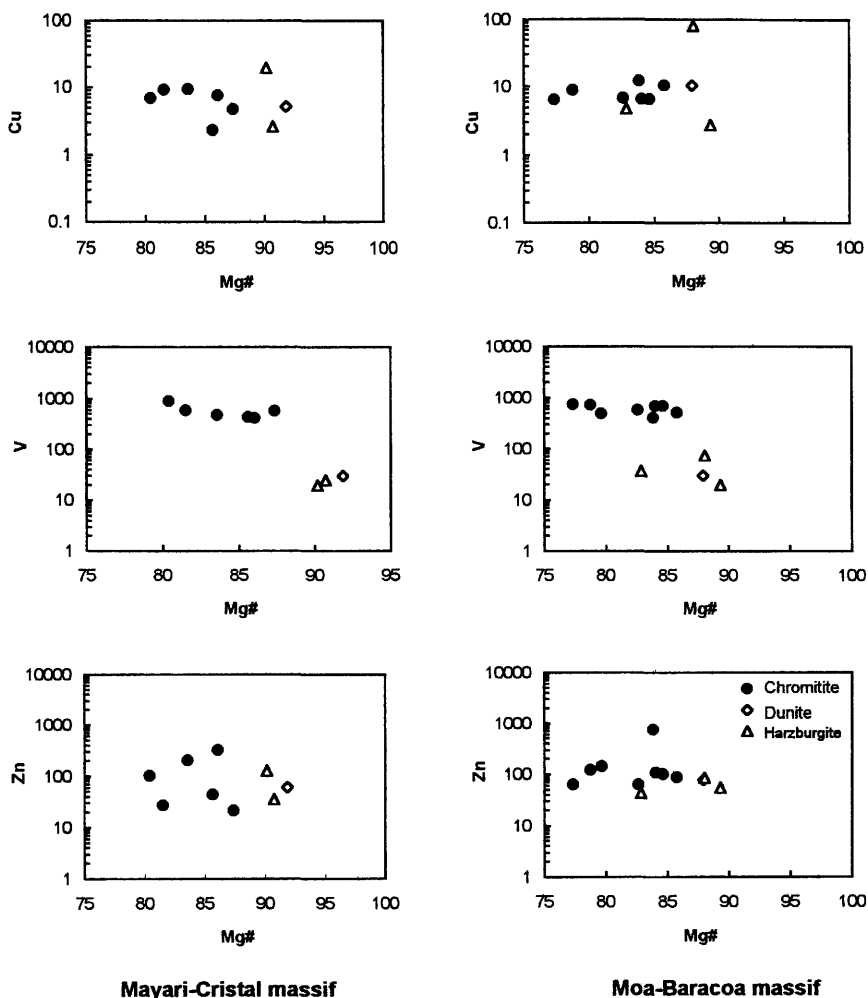


FIG. 4.  $Mg\# [MgO/(MgO+FeO)]$  versus V, Zn, and Cu of chromitites and ultramafic rocks from the Mayari-Baracoa ophiolite belt, eastern Cuba.

One massive chromitite (Cma2) from the MCM contains unusually high PGE contents reaching ore grade (total PGE content = 10 ppm, Ru = 5.6 ppm, and Ir = 2.0 ppm). Euhedral PGMs are abundant and enclosed in chromite grains in this sample, which, however, has a mantle-normalized PGE pattern similar to other chromitites (Fig. 5).

In both the MCM and MBM, Pt and Pd are generally positively correlated, whereas Pd and Ir are negatively correlated (Fig. 6). Chromitites have smaller Pd/Ir ratios than the silicate rocks. In Pd/Ir versus Ni/Cu plots, chromitites in the MCM have

higher Ni/Cu and smaller Pd/Ir ratios than those of the MBM (Fig. 7).

## Discussion

### *The MCM and MBM as a paired ophiolite belt*

It has been previously noted that the MCM and MBM differ in mineral chemistry and rock assemblages (Proenza et al., 1998, 1999b). The major rock type of the two massifs, harzburgite, is considered to represent a residuum after various degrees of partial melting. Experimental work has shown that the com-



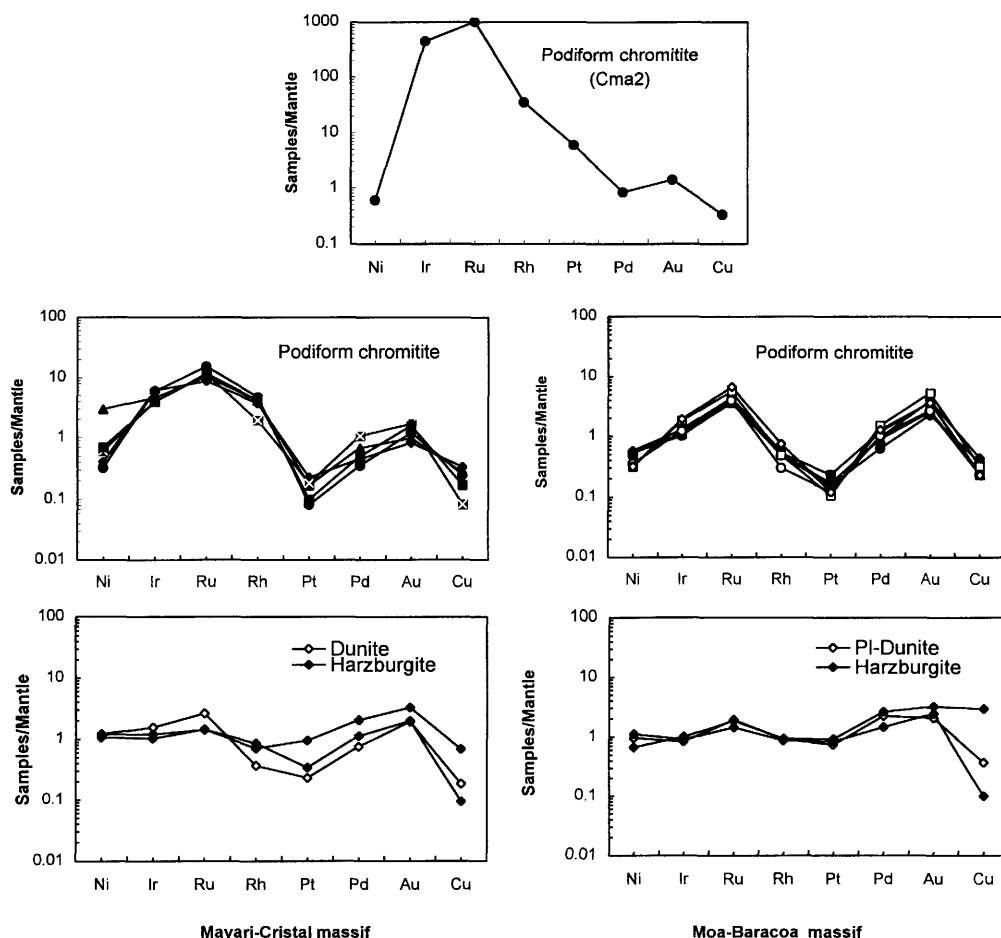


FIG. 5. Mantle-normalized Ni, PGE, Au, and Cu patterns of the chromitites and ultramafic rocks from the Mayari-Baracoa ophiolite belt, eastern Cuba. The normalization values are Ni 1950 ppm, Ir 4.4 ppb, Ru 5.6 ppb, Rh 1.6 ppb, Pt 8.3 ppb, Pd 4.4 ppb, and Cu 28 ppm (Barnes et al., 1987).

position of accessory chromite in this rock type changes and re-equilibrates with the associated olivine and pyroxene as melting proceeds (e.g., Mysen and Kushiro, 1977). In addition, higher Al in pyroxenes of the MBM harzburgite suggests lower degrees of partial melting compared to the MCM harzburgite. This is consistent with a lower Cr# for chromites in the former and a higher Cr# of chromite in the latter peridotites. The various degrees of depletion of the mantle peridotites suggests that both massifs represent one mantle section sampled at different levels, or that they are samples of mantle from distinct tectonic settings.

An upper mantle section is commonly thought to be stratified by progressive extraction of basaltic magmas, the most depleted residuum being the uppermost part (Nicolas, 1989). Comparing the ophiolite massifs to such a stratified section would suggest that the MCM represents the deeper portions of the column and the MBM the shallower portion, if they are part of the same mantle section as suggested by Proenza et al. (1999a). The high-Al chromitites are hosted in the MBM, which would have formed near the mantle-crust transition zone, and the high-Cr chromitites are hosted in the MCM, representing deeper mantle. However, the rock

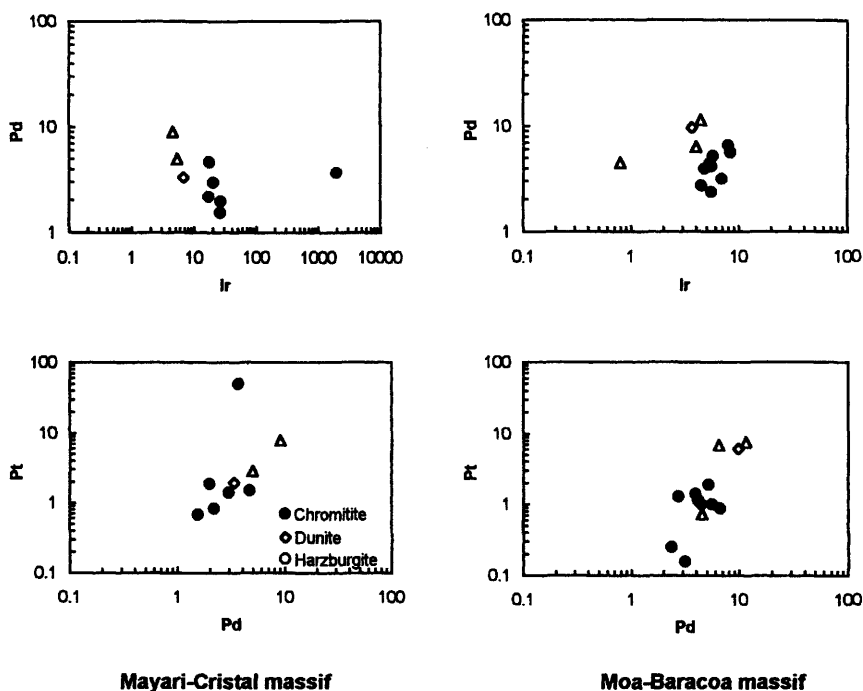


FIG. 6. Plots of Pt versus Pd and Ir versus Pd of the chromitites and ultramafic rocks from the Mayari-Baracoa ophiolite belt, eastern Cuba.

assemblages in both massifs do not support the concept that they represent parts of the same, stratified mantle column.

The MCM and MBM show different structural and geological features. There is considerably more dunite in the MCM, whereas in the MBM harzburgite is the dominant ultramafic rock. Plagioclase-bearing ultramafic rocks are a feature of the transition-zone rocks in the MBM, but the MCM does not have such lithologies. Gabbroic pegmatites cutting the chromitites and ultramafic rocks are abundant in the MCM, but are not found in the MBM. The MCM contains depleted harzburgites with high-Cr chromitites and pyroxenite dikes, whereas the MBM has high-Al chromitites and gabbroic and troctolitic dikes.

The pyroxenite dikes associated with the podiform chromitites might represent crystallization products of boninitic melts. Such boninitic melts most likely reflect hydrous mantle melting (Dick and Bullen, 1984) and formed by either high degrees of partial melting or by remelting of a progressively depleted source above a subduction zone (Crawford et al., 1989, and references therein). This

suggests that the MCM podiform chromitites were formed in a suprasubduction-zone environment.

Troctolite dikes are common in the mantle harzburgites of the East Pacific Rise, and have been interpreted as resulting from crystallization of MORB in the shallow mantle (Dick and Natland, 1996; Edwards and Malpas, 1996). A likely environment of formation for a rock assemblage of high-Al chromitite and troctolite, as in the MBM, is a back-arc spreading center.

The mineral compositions of chromitites are controlled by the compositions of magmas from which they crystallized, and it is now clear that high-Cr chromitites formed from boninitic magmas, and high-Al chromitites formed from tholeiitic magmas (Zhou and Robinson, 1994). In the MCM, the Cr# of accessory chromites in the harzburgite and dunite are the same as that of chromite in the chromitites, although they have lower Mg#. The high Cr# of the segregated chromite in the MCM is comparable to an origin of crystallization from a boninitic magma. As Proenza et al. (1999b) pointed out, the high-Al chromitite in the MBM crystallized from a tholeiitic magma and may have formed at relatively shallower

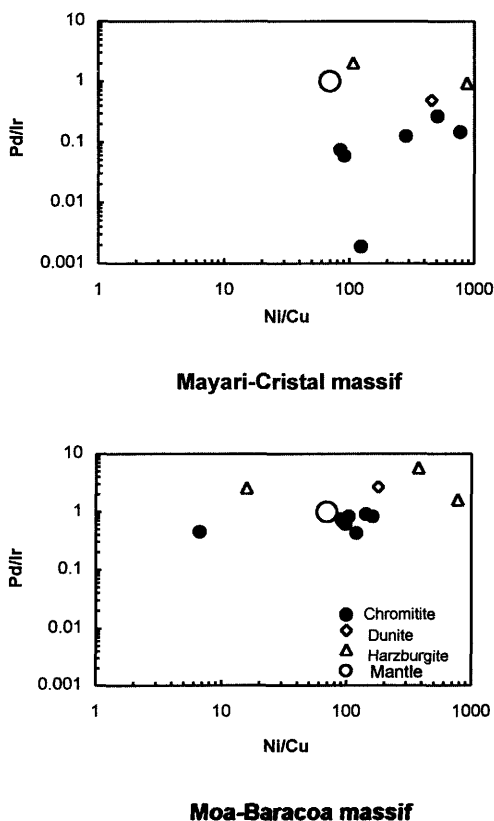


FIG. 7. Plots of Pd/Ir versus Ni/Cu of the chromitites and ultramafic rocks from the Mayari-Baracoa ophiolite belt, eastern Cuba.

depth. The higher Ti with higher Fe# of chromite of the MBM chromitites is probably controlled by the partial pressure of oxygen in the magmas, and must have formed at relatively shallow levels, i.e., at levels higher in the mantle than those at which low-Ti chromite crystallizes. This, therefore, does not support the idea of the MBM being a deeper portion of the same mantle column beneath the MCM. It is also unlikely for boninitic melts to evolve to tholeiitic melts either through vertical or subhorizontal movement, and thus to produce chromites of various compositions.

The geology and tectonic evolution of the northern Caribbean margin indicate that during the Upper Cretaceous, eastern Cuba was located above an intra-oceanic subduction zone (Lewis and Draper, 1990). The MCM and MBM may form a paired belt of mantle remnants beneath island-arc

(Aptian-Albian Volcanic Arc) and back-arc environments (Fig. 8), a situation similar to the Zambales ophiolites of the Philippines (Hawkins et al., 1984; Yumul, 1989; Zhou et al., 2000). An alternative view is that both ophiolitic massifs were formed in a forearc setting, where asthenospheric mantle was intruded into a lithospheric mantle (Malpas et al., 1997).

In either case, adjacent suprasubduction-zone environments would allow the formation of both types of podiform chromite deposits under oxidizing conditions (Roberts, 1988; Zhou and Robinson, 1997). In these sites, allochthonous magmas generated at different depths reacted with mantle peridotites, independently forming the two types of podiform bodies and associated rock types.

#### *PGE mineralization potential*

It has been noted that certain ophiolites may be PGE rich—for example, the Shetland ophiolite (Pritchard and Lord, 1993) and the Zambales ophiolite of the Philippines (Bacula et al., 1990). The PGE-rich units in these ophiolites are either mafic cumulates or podiform chromitites. Podiform chromitites are commonly enriched in iridium-subgroup PGE (IPGE, including Os, Ir, and Ru) relative to palladium-subgroup PGE (PPGE, including Rh, Pt, and Pd) in mantle-normalized plots (Zhou et al., 1998), and contain IPGE-dominated mineral, such as laurites and PGM alloys.

This type of mineralization occurs in eastern Cuba (Munoz Gomez, 1995; Proenza et al., 2001). Podiform chromitites from the MCM and MBM are also enriched in IPGE, although the former have higher PGE contents than the latter (Fig. 5). The enrichment of IPGE is believed to be derived from boninitic magmas that are S-undersaturated and enriched in these metals. To produce PGE-enriched magmas it is likely that a high degree of partial melting is responsible, inasmuch as this enables the removal of the very refractory PGE from the mantle. Barnes et al. (1985) suggested 20% partial melting of the mantle is required to consume all the sulfides. The high degree of melting ensures that these magmas are enriched in refractory elements such as Ni and Cr (Pearce et al., 1984), and maximizes the potential for the boninitic magma to be PGE enriched. Water derived from the downgoing slab not only promotes a high degree of partial melting required for the production of boninitic melts during the early stages of subduction, but it also facilitates the removal of PGE from the mantle. Boninitic mag-

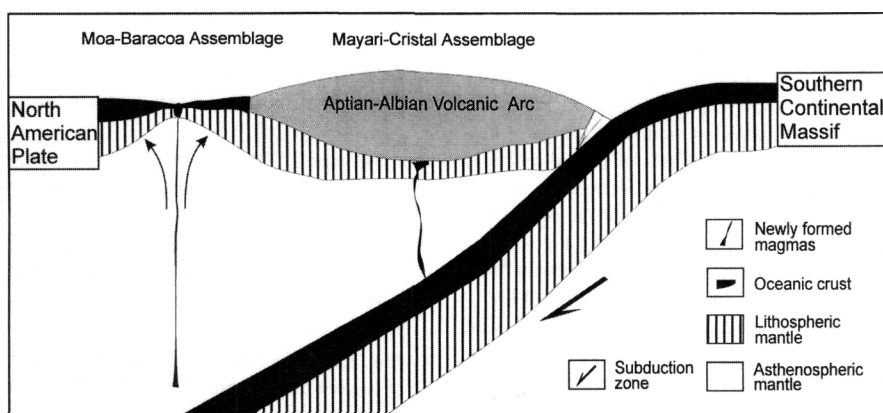


FIG. 8. Schematic plate-tectonic setting of the Mayari-Baracoa and Mayari-Cristal paired ophiolite belt, eastern Cuba.

mas provide the potential for PGE collection and concentration (e.g., Keays, 1995). For example, a PGE-rich boninitic magma provided a source for the PGE in the Bushveld layered igneous complex.

A chromitite, Cma2, from the MCM contains extremely high PGE contents (total PGEs over 10 ppm), and PGE minerals (alloys) are visible in individual chromite grains in thin section. However, all other elements seem to be indistinguishable from those in the other chromitites (Table 3 and Fig. 5). For example, Cma2 has similar Ni and Cu contents to other chromitites. This similarity would suggest that the enrichment of Ir and Ru was mainly the result of the presence of laurites and Ir-Ru alloys in the sample.

In addition to chromite, many metal alloys may also crystallize as early phases from a mafic magma. These phases are usually small in size and may not settle and concentrate on their own. The crystallization and settling of chromite therefore are crucial to the concentration of these metals. As a result, high-Cr chromitites are potentially important in the formation of PGE-enriched deposits. This fractionation of PGEs from the primary melts would have resulted in a Ni-, Cr-, and PGE-depleted magma which, on eruption, produced Ni, Cr, and PGE-depleted island-arc tholeiitic lavas.

### Conclusions

The Mayari-Cristal and Moa-Baracoa massifs in eastern Cuba have different rock associations and show distinct geochemical features, forming a paired ophiolite belt. The association of high-Al

chromites and troctolite dikes in the MBM suggest that they formed at lower pressure in a backarc spreading center, whereas the high-Cr chromitites in the MCM are closely associated with pyroxenite dikes, suggesting formation at higher pressures beneath an island arc. This study supports the concept that high-Cr chromitites crystallize from boninitic magmas, whereas high-Al chromitites are derived from tholeiitic magmas. The MCM has the potential for PGE mineralization.

### Acknowledgments

This study was initiated when three of the authors (MFZ, JL, and NMZ) attended an international field workshop meeting of IGCP 364 on Geological Correlation of Ophiolites and Volcanic Arc Terranes, held in eastern Cuba in 1996. Travel for MFZ to attend the meeting was supported by a HKU CRCG grant (to JM). W. Lavaut donated a number of specimens. The analytical work was substantially supported by grants from the Research Grant Council of Hong Kong Special Administrative Region, China (HKU7120/97P and HKU7301/99P to MFZ). We thank Ms. Ying Liu for skillful assistance with the analyses and Dr. Jianwei Li with the preparation of this manuscript.

### REFERENCES

- Bacuta, G. C., Kay, R. W., Gibbs, A. K., and Bruce, R. L., 1990, Platinum-group element abundance and distribution in chromite deposits of the Acoje Block, Zam-

- bales ophiolite complex, Philippines: *Journal of Geochemical Exploration*, v. 37, p. 113–145.
- Barnes, S.-J., Boyd, R., Korneliussen, A., Nilsson, L.-P., Often, M., Pedersen, R. B., and Robins, B., 1987, The use of mantle normalization and metal ratios in discriminating between the effects of partial melting, crystal fractionation and sulphide segregation on platinum-group elements, gold, nickel, and copper: Examples from Norway, in Prichard, H. M., Potts, P. J., Bowles, J. F. W., and Cribb, S. J., eds., *Geo-platinum Symposium volume*: London, Elsevier, p. 113–143.
- Barnes, S.-J., Naldrett, A. J., and Gorton, M., 1985, The origin of the fractionation of platinum-group elements in terrestrial magmas: *Chemical Geology*, v. 53, p. 303–323.
- Cobiella-Reguera, J., 2000, Jurassic and Cretaceous geological history of Cuba: *International Geology Review*, v. 42, p. 594–616.
- Crawford, A. J., Falloon, T. J., and Green, T. H., 1989, Classification, petrogenesis and tectonic setting of boninites, in Crawford, A. J., ed., *Boninites and related rocks*: London, Unwin Hyman, p. 1–49.
- Dick, H. J. B., and Bullen, T., 1984, Chromian spinel as a petrogenetic indicator in abyssal and alpine-type peridotites and spatially associated lavas: *Contributions to Mineralogy and Petrology*, v. 86, p. 54–76.
- Dick, H. J. B., and Natland, J. H., 1996, Last stage melt evolution and transport in the shallow mantle beneath the East Pacific Rise: Deep Sea Drilling Project, Initial Reports, v. 147, p. 103–134.
- Edwards, S. J., and Malpas, J., 1996, Melt-peridotite interactions in shallow mantle at the East Pacific Rise: Evidence from ODP Site 895 (Hess Deep): *Mineralogical Magazine*, v. 60, p. 191–206.
- Guild, P. W., 1947, Petrology and structure of the Moa chromite district, Oriente province, Cuba: *Transactions of the American Geophysical Union*, v. 28, p. 218–246.
- Hawkins, J. W., Bloomer, S. H., Evans, C. A., and Melchior, J. T., 1984, Evolution of intra-oceanic arc-trench systems: *Tectonophysics*, v. 102, p. 174–205.
- Iturralde-vinent, M. A., 1996, Geología de las ofiolitas de Cuba, in Iturralde-vinent, M. A., ed., *Ofiolitas y arcos volcanicos de Cuba*: IGCP Project 364, Special Contribution, no. 1, p. 83–120.
- Keays, R. R., 1995, The role of komatiitic and picritic magmatism and S-saturation in the formation of the ore deposits: *Lithos*, v. 34, p. 1–18.
- Kovacs, G. P., Buda, G., Watkinson, D. H., and Tompa, L., 1997, Chromite deposits of the Sagua-Baracoa Range, eastern Cuba: *Acta Geologica Hungarica*, v. 40, p. 337–353.
- Lewis, J. F., and Draper, G., 1990, Geological and tectonic evolution of the northern Caribbean margin, in Dengo, G., and Case, J. E., eds., *The geology of North America*, v. H, The Caribbean region: Boulder, CO, Geological Society of America, p. 77–140.
- Malpas, J., Robinson, P. T., and Zhou, M.-F., 1997, Chromitite and ultramafic rock compositional zoning through a paleotransform fault, Poom, New Caledonia—a discussion: *Economic Geology*, v. 92, p. 502–504.
- Munoz-Gomez, J. N., 1995, La paragenesis minerales del yacimiento Potosi y su sucesion genetica: *Revista Minería y Geología*, v. 12, p. 23–31.
- Mysen, B., and Kushiro, I., 1977, Compositional variations of coexisting phases with degree of melting of peridotite in the upper mantle: *American Mineralogist*, v. 62, p. 843–865.
- Nicolas, A., 1989, Structures of ophiolites and dynamics of oceanic lithosphere: Dordrecht, Netherlands, Kluwer Academic Publishers, 367 p.
- Pearce, J. A., Lippard, S. J., and Roberts, S. 1984, Characteristics and tectonic significance of suprasubduction zone ophiolites, in Kokelaar, B. P., and Howells, M. F., eds., *Marginal basin geology*: Geological Society of London, Special Publication no. 16, p. 77–94.
- Prichard, H. M., and Lord, R. A., 1993, An overview of the PGE concentrations in the Shetland ophiolite complex, in Prichard, H. M., Alabaster, T., Harris, N. B. W., and Neary, C. R., eds., *Magmatic processes and plate tectonics*: Geological Society of London, Special Publication no. 76, p. 273–294.
- Proenza, J., Gervilla, F., and Melgarejo, J. C., 1997, Compositional variations of podiform chromitites among different mining districts in the Mayari-Baracoa ophiolite belt (Eastern Cuba), in Papiunen, H., ed., *Mineral deposits*: Rotterdam, Netherlands, Balkema, p. 487–490.
- Proenza, J. A., Gervilla, F., and Melgarejo, J. C., 1999a, La Moho Transition Zone en el macizo ofiolítico Moa-Baracoa (Cuba): Un ejemplo de interacción magma/peridotita: *Revista Sociedad Geológicos España*, v. 12, p. 309–327.
- Proenza, J., Gervilla, F., Melgarejo, J. C., and Bodinier, J. L., 1999b, Al- and Cr-rich chromitites from the Mayari-Baracoa ophiolite belt (eastern Cuba): Consequence of interaction between volatile-rich melts and peridotites in suprasubduction mantle: *Economic Geology*, v. 94, p. 547–566.
- Proenza, J. A., Melgarejo, J. C., Gervilla, F., Lavant, W., Reve, D., and Rodriguez, G., 1998, Cromitites podiformes en La Faja Ofiolítica Mayari-Baracoa (Cuba): *Acta Geologica Hispanica*, v. 33, pp. 133–152.
- Proenza, J. A., Gervilla, F., Melgarejo, J. C., Vera, O., Alfonso, P., and Fallick, A., 2001, Genesis of sulfide-rich chromite ores by the interaction between chromitite and pegmatite olivine-norite dikes in the Potosi Mine (Moa-Baracoa ophiolite massif, Eastern Cuba): *Mineralium Deposita*, in press.
- Roberts, S., 1988, Ophiolitic chromitite formation: A marginal basin phenomenon?: *Economic Geology*, v. 83, p. 1034–1036.

- Sun, M., Jain, J., Zhou, M.-F., and Kerrich, R., 1993, A procedural modification for enhanced recovery of precious metals (Au, PGE) following nickel sulfide fire assay and tellurium co-precipitation: Applications for analysis of geological samples by inductively coupled plasma mass spectrometry: *Canadian Journal of Applied Spectrometry*, v. 38, p. 103–108.
- Thayer, T. P., 1942, Chrome resources of Cuba: U. S. Geological Survey Bulletin 935A, 74 p.
- \_\_\_\_\_, 1969, Gravity differentiation and magmatic replacement of podiform chromite deposits: *Economic Geology Monographs*, v. 4, p. 132–146.
- Yumul, G. P., Jr., 1989, Petrological characterization of the residual-cumulate sequences of the Zambales ophiolite complex, Luzon, Philippines: *Ophiolite*, v. 14, p. 253–291.
- Zhou, M.-F., and Robinson, P. T., 1994, High-Cr and high-Al chromitites, western China: Relationship to partial melting and melt/rock interaction in the upper mantle: *International Geology Review*, v. 36, p. 678–686.
- \_\_\_\_\_, 1997, Origin and tectonic setting of podiform chromite deposits: *Economic Geology*, v. 92, p. 259–262.
- Zhou, M.-F., Sun, M., Keays, R., and Kerrich, R., 1998, Controls on platinum-group elemental distributions of podiform chromitites: A case study of high-Cr and high-Al chromitites from Chinese orogenic belts: *Geochimica et Cosmochimica Acta*, v. 62, p. 677–688.
- Zhou, M.-F., Yumul, G. P., Jr., Malpas, J., and Sun, M., 2000, Comparative study of platinum-group elements in the Acoje and Coto blocks of the Zambales ophiolite, Philippines: *The Island Arc*, v. 9, p. 557–565.